nature geoscience

Article

https://doi.org/10.1038/s41561-022-01044-8

Negligible atmospheric release of methane from decomposing hydrates in mid-latitude oceans

Received: 27 January 2022

Accepted: 5 September 2022

Published online: 17 October 2022



Dong Joo Joung $oldsymbol{0}^{1,2} \boxtimes$, Carolyn Ruppel $oldsymbol{0}^3$, John Southon 4 , Thomas S. Weber $oldsymbol{0}^1$ and John D. Kessler $oldsymbol{0}^1$

Naturally occurring gas hydrates may contribute to a positive feedback for global warming because they sequester large amounts of the potent greenhouse gas methane in ice-like deposits that could be destabilized by increasing ocean/atmospheric temperatures. Most hydrates occur within marine sediments; gas liberated during the decomposition of seafloor hydrates or originating with other methane pools can feed methane emissions at cold seeps. Regardless of the origin of seep methane, all previous measurements of methane emitted from seeps have shown it to have a unique fossil radiocarbon signature, contrasting with other sources of marine methane. Here we present the concentration and natural radiocarbon content of methane dissolved in the water column from the seafloor to the sea surface at seep fields along the US Atlantic and Pacific margins. For shallower water columns, where the seafloor is not within the hydrate stability zone, we do document seep CH₄ in some surface-water samples. However, measurements in deeper water columns along the US Atlantic margin reveal no evidence of seep CH₄ reaching surface waters when the water-column depth is greater than 430 ± 90 m. Gas hydrates exist only at water depths greater than ~550 m in this region, suggesting that the source of methane escaping to the atmosphere is not from hydrate decomposition.

The rapid increase of atmospheric methane (CH₄) concentration observed over the past century is the product of both anthropogenic and natural emissions, as well as feedbacks associated with a warming climate $^{1-4}$. One potential feedback involves the thermal decomposition of gas hydrates, which represent a widespread and temperature sensitive methane reservoir of 1,800 GtC (×10 15 g) in CH₄ (ref. 5). Gas hydrate is found mostly in continental margin marine sediments in waters deeper than several hundred metres 5,6 . Contemporary ocean warming has the potential to trigger significant oceanic CH₄ release, especially along upper continental slopes on marine margins where

gas hydrates are barely within the pressure–temperature conditions for stability $^{\text{5-7}}\!.$

Beneath the seafloor, decomposing hydrates may supply some of the CH_4 emitted by seeps. Methane is released from seafloor seeps as visible, vapour phase bubbles and in the dissolved phase. The CH_4 contained in bubbles usually dissolves in the surrounding waters as the bubbles ascend (for example, refs. $^{8-11}$). Once dissolved, the concentration of CH_4 can be reduced through mixing with waters having lower CH_4 concentrations, transformation to CO_2 via aerobic microbial oxidation and/or release to the atmosphere via diffusion in near-surface

waters (for example, refs. $^{5,12-14}$). The efficiency of these processes depends on bubble characteristics (size or presence of surface coating such as oil or hydrate), the depth at which bubbles are released and environmental factors (for example, CH₄ concentrations in and temperatures of ambient ocean waters). Thus, water-column depth is an important parameter in controlling whether CH₄ emitted at seeps reaches the atmosphere or even near-surface waters. While models and measurements have investigated the influence of seep depth on the dissolution of bubbles during ascent (for example, refs. $^{8-11}$), in this Article, we directly fingerprint the source of CH₄ in surface waters at different total water-column depths. This enables the empirical determination of whether CH₄ originating at seeps, potentially sourced from hydrate decomposition, is escaping to the atmosphere in mid-latitude ocean basins.

In this study, we measured the concentration and natural radiocarbon content of CH₄ ([CH₄] and ¹⁴C-CH₄, respectively) dissolved in the water column within and near known seep fields along the US Atlantic margin (USAM) and US Pacific margin (USPM)¹⁵⁻¹⁹. All previously published measurements of ¹⁴C-CH₄ collected from natural seeps and dissociating hydrates have been fossil, which means devoid of measurable ¹⁴C (for example, refs. ²⁰⁻²⁵) (Table 1) and corresponding to an age older than approximately 60,000 years. However, there is no theoretical reason that more modern CH₄ could not be emitted in an as yet unmeasured seep. These fossil radiocarbon values for seep and hydrate CH₄ contrast with the modern values associated with CH₄ generated in the shallow water column by planktonic processes or produced in near-seafloor sediments via microbial breakdown of younger organic carbon^{21-24,26,27}. In some settings, CH₄ in sediments adjacent to seafloor seeps can even have modern 14C values while the nearby seeps release fossil CH₄ (Table 1)²¹.

The measurements reported here are consistent with seep CH_4 being a fossil radiocarbon endmember and CH_4 in the shallow water column having measurable (modern) radiocarbon. This enables us to apply a ^{14}C – CH_4 mixing model that exploits the fossil ^{14}C signal of seep CH_4 to constrain the fraction of dissolved (water column) CH_4 that is sourced from seeps 14 . The samples collected here for natural radiocarbon analysis spanned total water-column depths that in some cases bracketed the shallow pressure–temperature limit for CH_4 hydrate stability. This provides us with an additional opportunity to examine the fate of fossil seep CH_4 that may have originated with dissociating gas hydrates.

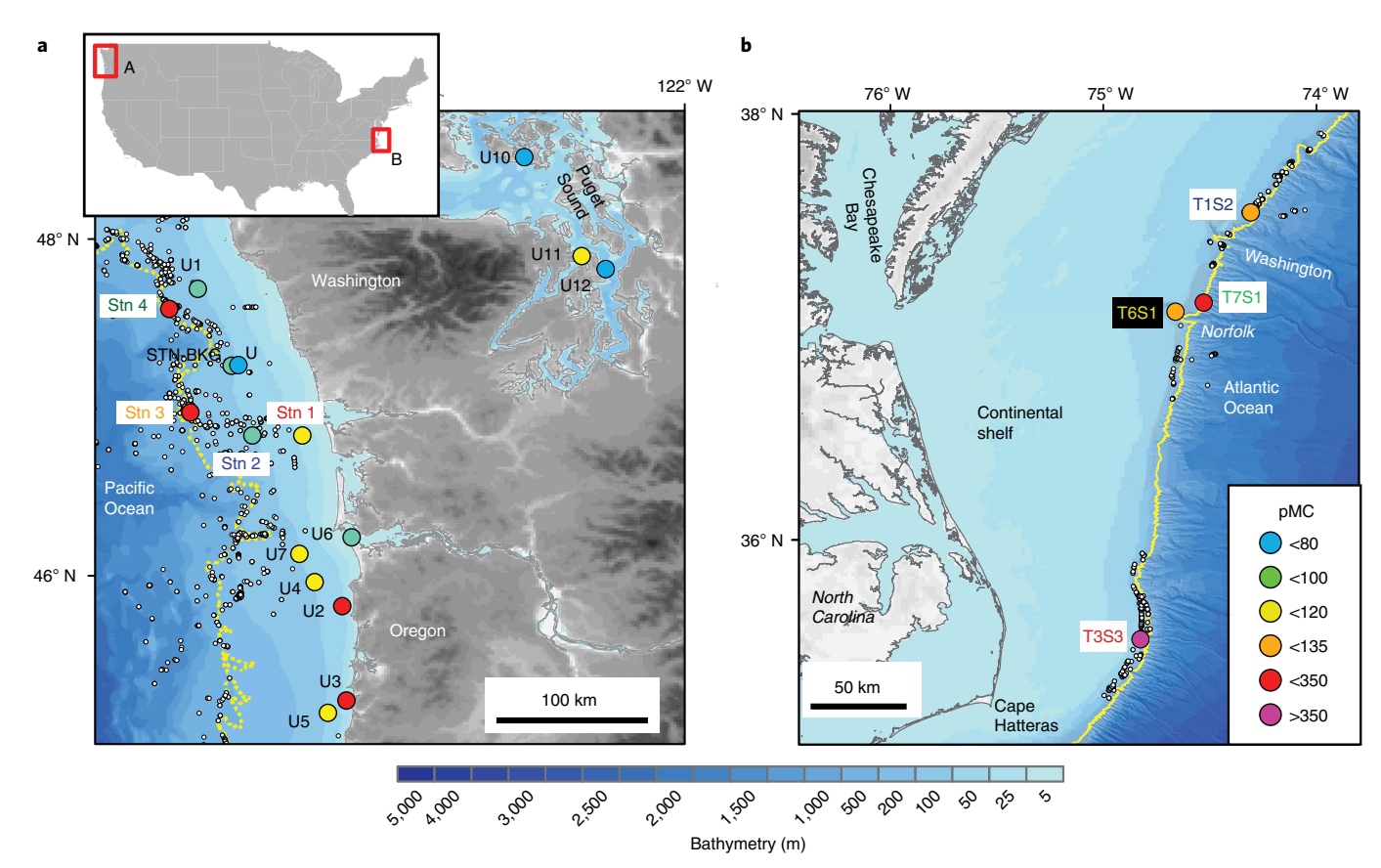
Upper continental slope sites

On the USAM between 35.53° and 37.54° N, we collected water-column samples at upper continental slope locations with water depths of 300-600 m, which brackets the nominal upper boundary for stability of pure CH₄ gas hydrate (~550 m) on this margin⁵ (Fig. 1). Samples were collected at several discrete depths from near the seafloor to near the sea surface at four stations with and without seafloor seepage between Cape Hatteras and just north of Washington Canyon. At three of these stations (T3S3, T6S1 and T7S1), the deepest sample collected was ~100 m shallower than the nominal landward limit of gas hydrate stability at ~550 m. The station north of Washington Canyon (T1S2) was in significantly shallower waters (288 m) but in an area of pervasive CH₄ seepage^{13,28}. At stations T1S2, T3S3 and T7S1, values of ¹⁴C-CH₄ dissolved in bottom waters (288–400 m) varied from 0.1 to 6.9 percent modern carbon (pMC) (Fig. 2), indicating that these seep fields emit fossil CH4. At station T6S1, the deepest sample measured had a ¹⁴C-CH₄ value of 55 pMC (Fig. 2), but this sample was collected ~100 m above the seafloor where seep and background CH₄ may be mixed (Figs. 1 and 2). At the station designated as 'background' (T7S1) due to no visible bubble emissions in our acoustic surveys, or in previous surveys (Extended Data Fig. 1 and ref. 14), the deepest sample, which was acquired 100 m above the seafloor, had an unexpectedly low 14C-CH₄ value: 2.5 pMC. This sample was collected adjacent to Norfolk Canyon, one of the major

Table 1 | Δ¹⁴C-CH₄ values in seep gas, gas hydrate, sediments and deep water immediately above the seep

Location	CH₄ form	¹⁴ C-CH ₄ (pMC)	Note	Reference
Santa Barbara	Seep gas	0.04±0.06	n=8	22
Guaymas Basin	Seep gas	0.2±0.1	n=11	22
Guaymas Basin	Seep gas	0.24	n=3, excavation vent	22
Bullseye Vent, Cascadia margin	Seep gas	1.68-2.24	n=3	23
Barkley Canyon, Cascadia margin	Seep gas	0.85-1.17	n=2	23
Concepción Seep, Chilean margin	Seep gas	<0.12-0.14	n=3	23
Cascadia Margin/Bullseye Vent	Seep gas	4.38±1.14	n=3	23
Black Sea	Seep gas	5.0±0.4		45
Hydrate Ridge, Cascadia margin	Gas hydrate	0.24	n=3	25
Guaymas Basin, Gulf of California	Gas hydrate	0.29	Gas hydrate + sediment gas	22
Bullseye Vent, Cascadia margin	Gas hydrate	<0.12-1.48	n=3	23
Barkley Canyon, Cascadia margin	Gas hydrate	<0.12-1.17	n=5	23
Concepción Seep, Chilean margin	Gas hydrate	<0.12	n=1	23
Green Canyon, Gulf of Mexico	Gas hydrate	<0.12	n=3	23
Blake Ridge, Blake Ridge	Gas hydrate	<0.12	n=2	23
Haakon Mosby Mud Volcano, Norwegian Sea	Gas hydrate	<0.12	n=1	23
Bush Hill, Gulf of Mexico	Gas hydrate	2.11±0.32	n=3	20
Cariaco Basin	Sediment CH ₄	86.4	at 45cm depth	21
Santa Barbara	Sediment CH ₄	67-86.4	at 45–50 cm depth	22
Skan Bay	Sediment CH ₄	>88	surface to 73 cm depth	22
USAM-Hudson Canyon*	Sediment CH ₄	73	2,505 years before present in ¹⁴ C age	46
USAM- Chincoteague*	Sediment CH₄	12.7-27.6	16,520– 10,350 years before present in ¹⁴ C age, deep-water seep field ~1,100 m	46
USAM	Deep water	0.1	Right above the seep at 288 m depth (T1S2)	This stud

^{*14}C-CH₄ values were converted from ¹⁴C ages.



 $\label{eq:Fig.1} \textbf{Summary of surface-water} \ ^{14}\textbf{C-CH}_4 \ results. \ a,b, \ \text{Results with units of pMC collected from near-surface waters in the Pacific Northwest (a) and the Mid-Atlantic Bight (b), in areas A and B, respectively, highlighted by the red boxes on the inset map. Salish Sea connects waters from the Pacific Ocean and Puget Sound, located between Washington, USA, and Vancouver Island, Canada, in a. Known seep locations are shown as white circles $^{15,16,18,31-33,47}$. Yellow curves indicate$

the approximate landward limit of gas hydrate as determined from near-bottom temperature measurements for the Pacific Northwest and corresponding to the 550 m isobath on the Mid-Atlantic margin⁴⁸. Note that Phrampus³⁴ reported the hydrate stability depth as 480 m in Cascadia margin, Pacific Ocean. Station labels are colour coded to match those in Figs. 2 and 3.

shelf-break canyons in the mid-Atlantic Bight, and was probably influenced by undocumented fossil CH_4 seep emissions in the area or by ephemeral seeps not emitting methane at the time of our sampling.

In the intermediate part of the water column, which we define as depths between the deepest sample and surface waters, all samples had $^{14}\text{C-CH}_4$ values more elevated (higher pMC) than the bottom waters but considerably lower than contemporary values. In general, the pMC for $^{14}\text{C-CH}_4$ from intermediate depths increased with shallower depths in the water column (Fig. 2). This pattern is expected since most fossil CH $_4$ originating with seep emissions dissolves close to the seafloor and is only rarely carried by bubbles to high altitudes above the seafloor 9,10 .

In contrast to the respectively strong (<10 pMC) and weaker (-20-100 pMC) fossil CH₄ signatures in near-bottom and intermediate-depth waters, USAM surface-water $^{14}\text{C}-\text{CH}_4$ values were almost entirely modern and within the range previously reported in aquatic environments 22,24,29 . These modern $^{14}\text{C}-\text{CH}_4$ values reflect equilibration of surface waters with the contemporary atmosphere and water-column aerobic methanogenesis from modern carbon sources 13,27 . The lack of fossil radiocarbon in surface waters indicates that fossil CH₄ from seeps is not being transported to these surface waters or emitted to the atmosphere at these locations. Leonte et al. 12 estimated that CH₄ oxidation in Hudson Canyon, at the northern end of the mid-Atlantic Bight and $^{-3}$ 300 km north of our sampling area, could be as fast as 62.7 \pm 37 nM d $^{-1}$, with more than half of seep CH₄ released into the overlying water column being oxidized within that specific seep field. At sites investigated here, microbial oxidation probably contributes

substantially to the removal of fossil CH_4 injected into the water column across the sediment–water interface. However, transport by ocean currents (for example, ref. 30) and subsequent dilution could also play a significant role in the apparent removal of fossil CH_4 . To investigate this possibility, we applied a two-endmember mixing model. The results demonstrated that much of the vertical variation in the radiocarbon and concentration values could be described as mixing between seep-derived and background CH_4 (Extended Data Fig. 2). This model suggests that, in addition to the oxidation sink, water mixing plays a significant role in decreasing the concentration of dissolved CH_4 .

Shallow continental-shelf sites

Along the USPM, we sampled the water column at continental-shelf and uppermost slope sites (maximum water depth 226 m) to constrain the water depth for which fossil CH₄ emitted at the seafloor first becomes observable in surface waters. Like in previous studies (for example, refs. $^{3i-33}$), we detected many water-column bubble flares reaching at least 10–20 m above the seafloor during our cruise's hydroacoustic surveys (Extended Data Fig. 3). Although these continental-shelf seeps are too shallow to tap dissociating gas hydrate (nominal top of hydrate stability ~480 m (ref. 34)), they could be fed by several sources of CH₄, including CH₄ generated in situ in shallow sediments, CH₄ migrating from deep hydrocarbon reservoirs and CH₄ transported to the shelf by rivers and submarine groundwater discharge.

Bottom-water ¹⁴C-CH₄ measurements at five locations along the USPM ranged from 16 to 170 pMC, with only two values being

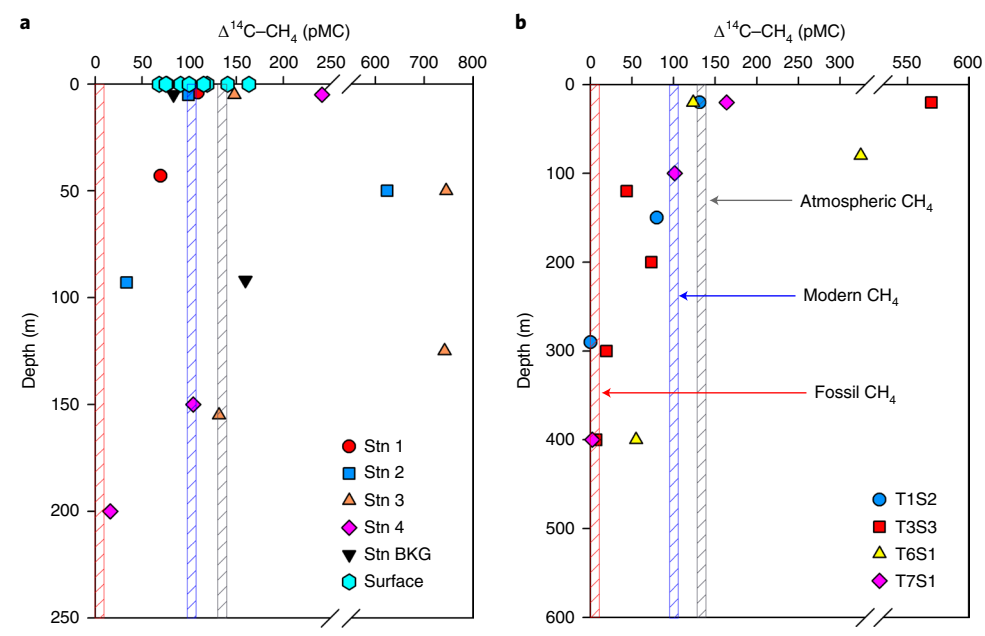


Fig. 2 | **Vertical profiles of Δ^MC-CH₄. a,b**, The profiles in the USPM (**a**) and USAM (**b**). Interestingly, the vertical profile of 14 C-CH₄ at station T3S3 in USAM displayed a lower value at 120 m depth (43 pMC) than at 200 m depth (73 pMC). Acoustic measurements at this station revealed that there was a scattering layer of bubbles or particles at this mid-depth, probably capping the submarine canyon (Extended Data Fig. 1). Because the value at 200 m seemed in line with the general trendline of increasing 14 C-CH₄ values with decreasing depth (Extended

Data Fig. 2), the low value of ${}^{14}\text{C}-\text{CH}_4$ at 120 m is probably an intrusion of older CH $_4$ carbon associated with this acoustic anomaly. Some ${}^{14}\text{C}-\text{CH}_4$ values were extremely high, displaying values four to five times those of the contemporary atmosphere and about two times the highest value reported earlier 22 . These high values (>140 pMC) were probably associated with nuclear activities and were discussed fully in a separate article 49 .

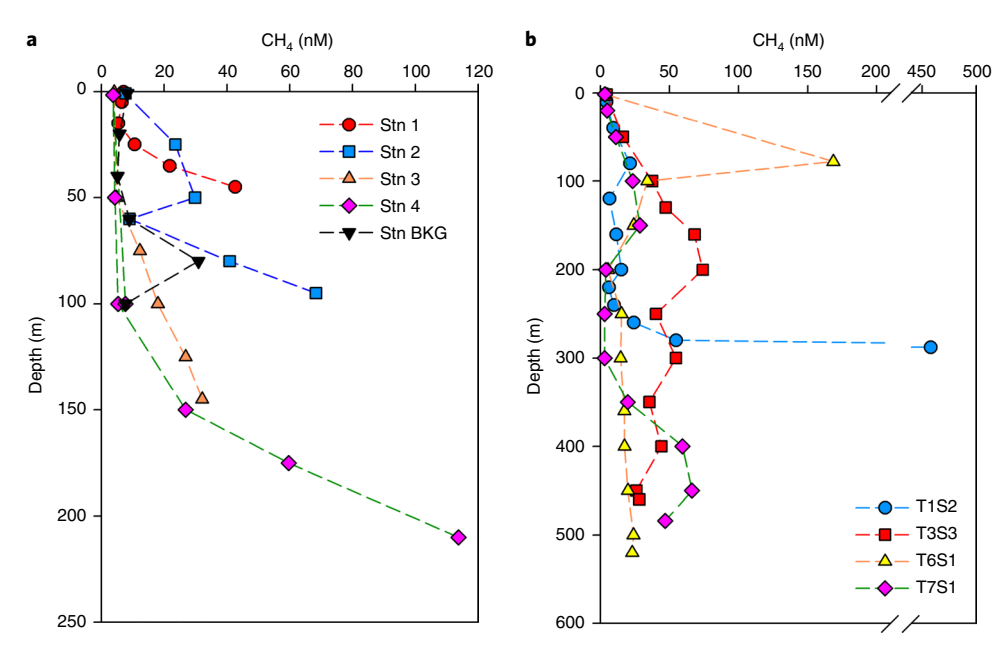


Fig. 3 | Vertical profiles of dissolved CH₄ concentration. a,b, The CH₄ concentration values in the USPM (a) and USAM (b). Distribution of surface CH₄ concentrations is available in Extended Data Fig. 4. Vertical distributions of the ancillary data are shown in Extended Data Fig. 7.

contemporary (100 pMC) or even higher. At the deepest (226 m) site (Stn 4), the bottom water had a $^{14}\text{C}-\text{CH}_4$ value of 16 pMC, which was the lowest value measured on this margin. This $^{14}\text{C}-\text{CH}_4$ sample was collected -26 m above the seafloor, implying that the near-bottom water at this location probably had a fossil (-0 pMC) signature due to the numerous nearby seafloor seeps (Extended Data Fig. 3). At Stn 1,

a well-known shallow-water (-50 m) CH $_4$ seep site (for example, ref. 16 and references therein 17,19), bottom-water 14 C–CH $_4$ was 70 pMC, probably reflecting a mixture of seep (fossil) CH $_4$ and modern sediment and water-column CH $_4$ (Supplementary Text).

Values of 14 C-CH₄ dissolved in surface waters of the USPM varied from 68 to 241 pMC, with 75% and 40% of the samples at or below the

modern contemporary values of atmospheric CH₄ (~135 pMC) and organic matter (100 pMC), a precursor for CH₄, respectively (Supplementary Table 1). The low 14C-CH₄ (<100 pMC) surface values were observed only at the shallowest sites on the shelf (<110 m water-column depth at Stn BKG, U1 and U8) and the inner water bodies of the Salish Sea (<165 m water-column depth at U10 and U12) (Fig. 1). Geochemical and isotopic signatures can sometimes provide clues about these CH₄ sources. For example, station U10 along the USPM displayed high concentrations of CH₄ and nitrate and low dissolved oxygen concentrations at the surface, probably reflecting the inputs of groundwater or upwelling of bottom water influenced by seepage (Extended Data) Fig. 4). However, considering the acoustic detection of numerous seeps along the cruise track (Extended Data Fig. 3) and that these seeps emit fossil CH₄ (Table 1) in contrast to the modern values of ¹⁴C-CH₄ recorded at the Columbia River mouth (~100 pMC at U6) and in typical sediments^{22,23,35}, the lower pMC values of ¹⁴C-CH₄ observed in some surface waters investigated in this region (Stn BKG, U1, U8 and U12) were probably affected by fossil CH₄ emitted from seafloor seeps. Thus, fossil CH₄ emitted from seafloor seeps at water depths up to 200 m on the USPM continental shelf is probably reaching the sea-air interface at some locations.

Fossil methane detection in surface waters

While some surface waters sampled from the USPM continental shelf showed signals from benthic (fossil) CH₄ inputs, all USAM surface samples and most of those from the USPM had values of ¹⁴C-CH₄ that were equal to or greater than 100 pMC. Even at relatively shallow sites with water depths ranging from 100 to 300 m (all USPM sites and one USAM site), CH₄ dissolved in surface waters was predominately modern. Entirely modern CH₄ in ocean surface waters above the seafloor within 100 m of the upper stability boundary for hydrates on the USAM implies that seeps fuelled by hydrate decomposition do not influence oceanic CH₄ emissions to the atmosphere in such settings. Conversely, the detection of a larger fossil CH₄ signature in surface waters at some USPM continental-shelf locations with total water-column depth greater than 100 m implies that a fraction of the CH₄ emitted from shallow-water seafloor seeps may reach the sea-air interface, although we emphasize that such water depths are too shallow for gas hydrates to be present in the sediments.

We correlated the fraction of dissolved CH₄ that is sourced from seeps versus altitude above the seafloor to determine the water depths at which fossil CH₄ is detectable in ocean surface waters (Fig. 4). This analysis incorporates only results from the USAM, where samples were acquired at intermediate and near-bottom water-column depths not influenced by atmospheric mixing. In this analysis, 'seep fraction' is defined as one minus the ratio of measured to contemporary ¹⁴C-CH₄. Contemporary CH₄ is defined as ranging from modern carbon (100 pMC) to atmospheric CH₄ (135 pMC). The analysis reveals a linear relationship between the fraction of fossil CH₄ and altitude (height above the sea bottom), indicating that fossil CH₄ is not detectable in surface waters with a total water-column depth of 430 ± 90 m (Fig. 4), which is shallower than the nominal upper stability boundary for gas hydrates on the USAM (~550 m (ref. 36)). This depth distribution of fossil CH₄ is in agreement with previous models of CH₄ dissolution from bubbles emitted at seafloor seeps (for example, refs. 8-11,37,38). While this linear correlation suggests that fossil CH₄ should be detectable in surface waters with water-column depths shallower than ~350 m, none of the USAM (continental slope) or USPM (continental shelf) surface-water samples has ¹⁴C-CH₄ values below 100 pMC until the water-column depth is 164 m or less (Fig. 5).

In summary, our 14 C-CH $_4$ measurements indicate that CH $_4$ in bottom waters along the upper continental slope of the USAM and continental shelf and uppermost continental slope of the USPM contain fossil CH $_4$ derived from seafloor seeps. Within the water column, the fossil radiocarbon values and [CH $_4$] are diminished relative to

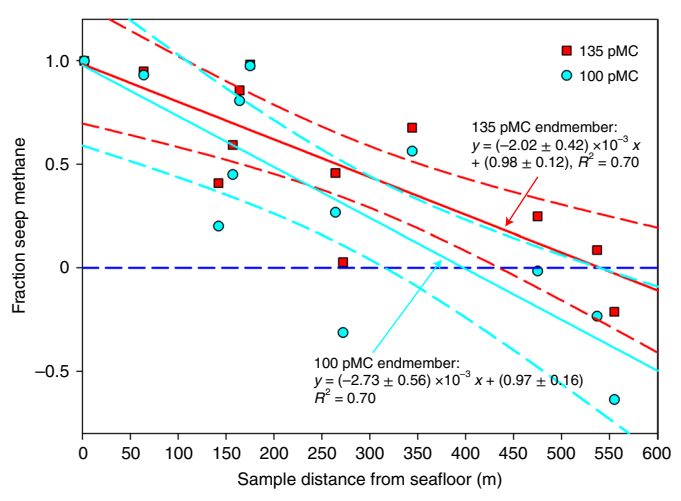
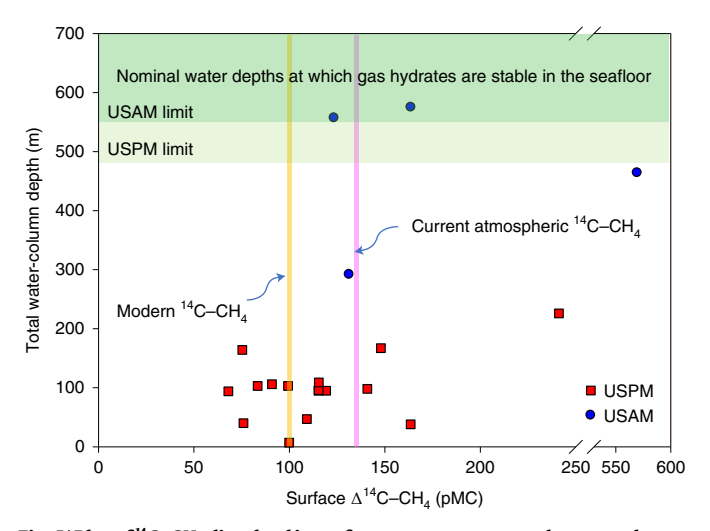


Fig. 4 | **The distribution of the fraction of seep CH**₄ **dissolved in waters as a function of altitude above the seafloor.** The fraction of seep CH₄ was determined using ${}^{14}\text{C}-\text{CH}_4$ values from the USAM data as described in the text. Red rectangles and line assume that a ${}^{14}\text{C}-\text{CH}_4$ value of 135 pMC contains no seep CH₄. Cyan dots and line assume that a ${}^{14}\text{C}-\text{CH}_4$ value of 100 pMC contains no seep CH₄. Two values that were influenced by nuclear power effluents (570 and 325 pMC) were omitted from this analysis 49 . Based on these two possible endmembers and including the uncertainty in the linear least squares region of the data, the altitude above the seafloor where no fossil (seep) CH₄ remains is 430 \pm 90 m. Since the upper stability boundary for gas hydrates is -550 m depth on this margin, this provides empirical evidence that seep CH₄ released from decomposing hydrates is unlikely to be emitted to the atmosphere in these regions. All analytical errors are smaller than the data points in the figure.



 $\label{eq:Fig.5} \textbf{Plot of }^{\text{H}}\textbf{C}-\textbf{CH}_4 \ dissolved \ in surface \ waters \ versus \ total \ water-column \ depth \ where \ the \ samples \ were \ collected. This \ figure \ displays \ that \ no \ surface-water \ samples \ display \ fossil \ CH_4, \ or \ any \ CH_4 \ with \ a^{14}\textbf{C}-\textbf{CH}_4 \ value \ below \ the \ contemporary \ atmosphere \ or \ modern \ carbon, \ until \ the \ total \ water-column \ depth \ is less \ than \ or \ equal \ to \ 164 \ m.$

benthic waters, showing increasing pMC 14 C-CH₄ values and decreasing concentrations due to rapid oxidation and mixing. Some surface waters at USPM continental-shelf sites (water depth < 200 m) have relatively low pMC 14 C-CH₄, suggesting that seafloor CH₄ emissions are contributing a minor fraction of fossil CH₄ to the ocean surface and the atmosphere. However, these water depths are too shallow for gas hydrate decomposition to be contributing to fossil CH₄, and our analysis cannot distinguish whether fossil CH₄ in the surface waters at

these sites originates from seeps or submarine groundwater discharge. Most important, since no fossil seep CH_4 is detectable in USAM surface waters where the water depth is 430 ± 90 m, which is shallower than the upper stability boundary for gas hydrates in this region, any fossil CH_4 detected in surface waters is unlikely to be sourced in the thermal decomposition of gas hydrates.

While we cannot trace the fossil CH_4 we observed at the seafloor to a specific seep where hydrate dissociation is occurring, our results imply that CH_4 released at the depths where this process occurs in mid-latitudes does not reach the atmosphere. These empirical results are supported by previous modelling investigations (for example, refs. \$-11,37,38), which also found that CH_4 from deep seeps and hydrate dissociation in mid-latitude oceans is unlikely to reach the sea surface. In some Arctic Ocean waters, the upper stability boundary for gas hydrates occurs shallower than the 430 ± 90 m threshold depth reported here 5,6 ; thus, more extensive study would be needed to test whether the conclusions we have drawn for mid-latitudes also apply to high-latitude regions 24 .

Recently, the Intergovernmental Panel on Climate Change² reported an updated global CH₄ budget including both top-down and bottom-up estimates of CH₄ sources. In that report, the bottom-up estimates of hydrate-derived CH₄ emissions to the atmosphere are $4-10 \text{ Tg y}^{-1}$ (ref. ³⁹) out of the total geological emissions of ~52 Tg yr⁻¹ CH_4 (refs. ^{2,40,41}), with potential to increase with further warming ⁴². An analysis of the panel's first five reports indicated that the presumed atmospheric fluxes for hydrate-derived CH₄ were based mostly on faulty assumptions⁵, and our findings here indicate that hydrates are negligible sources of atmospheric methane in mid-latitudes. Our findings of absent or low fossil CH₄ in shallow ocean surface waters on the upper continental slope of the USAM and continental shelf of the USPM strongly suggest that the oceanic emission of hydrate CH₄ to the atmosphere is non-existent at temperate latitudes, thereby providing empirical evidence to support previous conclusions (for example, refs. ^{5,8–11,13,16,24,37,38,40–44}). Furthermore, at continental slope sites, the disappearance of a water-column fossil CH₄ signature within a few hundred metres above the seafloor implies that, even if gas hydrate dissociation accelerates with future warming, this source of seep CH₄ is unlikely to be transported to surface waters or emitted to the atmosphere.

Online content

Any methods, additional references, Nature Research reporting summaries, source data, extended data, supplementary information, acknowledgements, peer review information; details of author contributions and competing interests; and statements of data and code availability are available at https://doi.org/10.1038/s41561-022-01044-8.

References

- Anthony, K. M., Anthony, P., Grosse, G. & Chanton, J. Geologic methane seeps along boundaries of Arctic permafrost thaw and melting glaciers. *Nat. Geosci.* 5, 419–426 (2012).
- Canadell, J. G. et al. in Climate Change 2021: The Physical Science Basis (eds Masson-Delmotte, V. et al.) Ch. 5 (Cambridge Univ. Press, 2021).
- Reeburgh, W. S. Oceanic methane biogeochemistry. Chem. Rev. 107, 486–513 (2007).
- Tarnocai, C. et al. Soil organic carbon pools in the northern circumpolar permafrost region. Glob. Biogeochem. Cycles https:// doi.org/10.1029/2008gb003327 (2009).
- Ruppel, C. D. & Kessler, J. D. The interaction of climate change and methane hydrates. Rev. Geophys. 55, 126–168 (2017).
- Ruppel, C. D. Methane hydrates and contemporary climate change. Nat. Educ. Knowl. https:// www.nature.com/scitable/knowledge/library/ methane-hydrates-and-contemporary-climate-change-24314790/ (2011).

- 7. Buffett, B. & Archer, D. Global inventory of methane clathrate: sensitivity to changes in the deep ocean. *Earth Planet. Sci. Lett.* **227.** 185–199 (2004).
- Rehder, G., Leifer, I., Brewer, P. G., Friederich, G. & Peltzer, E. T. Controls on methane bubble dissolution inside and outside the hydrate stability field from open ocean field experiments and numerical modeling. *Mar. Chem.* 114, 19–30 (2009).
- 9. Leonte, M. et al. Using carbon isotope fractionation to constrain the extent of methane dissolution into the water column surrounding a natural hydrocarbon gas seep in the northern Gulf of Mexico. *Geochem. Geophys. Geosyst.* **19**, 4459–4475 (2018).
- Wang, B., Jun, I., Socolofsky, S. A., DiMarco, S. F. & Kessler, J. D. Dynamics of gas bubbles from a submarine hydrocarbon seep within the hydrate stability zone. *Geophys. Res. Lett.* https://doi. org/10.1029/2020ql089256 (2020).
- Fu, X., Waite, W. F. & Ruppel, C. D. Hydrate formation on marine seep bubbles and the implications for water column methane dissolution. J. Geophys. Res. Oceans 126, e2021JC017363 (2021).
- Leonte, M. et al. Rapid rates of aerobic methane oxidation at the feather edge of gas hydrate stability in the waters of Hudson Canyon, US Atlantic Margin. Geochim. Cosmochim. Acta 204, 375–387 (2017).
- Leonte, M., Ruppel, C. D., RuizAngulo, A. & Kessler, J. D. Surface methane concentrations along the Mid-Atlantic Bight driven by aerobic subsurface production rather than seafloor gas seeps. J. Geophys. Res. Oceans https://doi.org/10.1029/2019jc015989 (2020).
- Joung, D. et al. Radiocarbon in marine methane reveals patchy impact of seeps on surface waters. *Geophys. Res. Lett.* https://doi. org/10.1029/2020ql089516 (2020).
- Baldwin, W. E., Moore, E. M., Worley, C. R., Nichols, A. R. & Ruppel, C. D. Marine Geophysical Data Collected to Support Methane Seep Research Along the US Atlantic Continental Shelf Break and Upper Continental Slope Between the Baltimore and Keller Canyons (USGS, 2020); https://doi.org/10.5066/P9Y1MSTN
- Johnson, H. P., Miller, U. K., Salmi, M. S. & Solomon, E. A. Analysis of bubble plume distributions to evaluate methane hydrate decomposition on the continental slope. *Geochem. Geophys.* Geosyst. 16, 3825–3839 (2015).
- Seabrook, S., De Leo, F. C., Baumberger, T., Raineault, N. & Thurber, A. R. Heterogeneity of methane seep biomes in the Northeast Pacific. *Deep Sea Res.* 2 150, 195–209 (2018).
- Skarke, A., Ruppel, C., Kodis, M., Brothers, D. & Lobecker, E.
 Widespread methane leakage from the sea floor on the northern US Atlantic margin. *Nat. Geosci.* 7, 657–661 (2014).
- Torres, M. E. et al. Methane sources feeding cold seeps on the shelf and upper continental slope off central Oregon, USA. Geochem. Geophys. Geosyst. 10, Q11003 (2009).
- Grabowski, K. S. et al. Carbon pool analysis of methane hydrate regions in the seafloor by accelerator mass spectrometry. *Nucl. Instrum. Methods Phys. Res. B* 223–224, 435–440 (2004).
- Kessler, J. D., Reeburgh, W. S., Southon, J. & Varela, R. Fossil methane source dominates Cariaco Basin water column methane geochemistry. *Geophys. Res. Lett.* https://doi. org/10.1029/2005gl022984 (2005).
- Kessler, J. D. et al. A survey of methane isotope abundance (¹⁴C, ¹³C, ²H) from five nearshore marine basins that reveals unusual radiocarbon levels in subsurface waters. *J. Geophys. Res. Oceans* https://doi.org/10.1029/2008jc004822 (2008).
- 23. Pohlman, J. W. et al. Methane sources in gas hydrate-bearing cold seeps: evidence from radiocarbon and stable isotopes. *Mar. Chem.* **115**, 102–109 (2009).
- Sparrow, K. J. et al. Limited contribution of ancient methane to surface waters of the US Beaufort Sea shelf. Sci. Adv. 4, eaao4842–eaao4842 (2018).

- Winckler, G. et al. Noble gases and radiocarbon in natural gas hydrates. Geophys. Res. Lett. https://doi.org/10.1029/ 2001GL014013 (2002).
- Karl, D. M. et al. Aerobic production of methane in the sea. Nat. Geosci. 1, 473–478 (2008).
- Repeta, D. J. et al. Marine methane paradox explained by bacterial degradation of dissolved organic matter. *Nat. Geosci.* 9, 884–887 (2016).
- Garcia-Tigreros, F. et al. Estimating the impact of seep methane oxidation on ocean pH and dissolved inorganic radiocarbon along the US mid-Atlantic Bight. J. Geophys. Res. Biogeosci. 126, e2019JG005621 (2021).
- Joung, D., Leonte, M. & Kessler, J. D. Methane sources in the waters of Lake Michigan and Lake Superior as revealed by natural radiocarbon measurements. *Geophys. Res. Lett.* 46, 5436–5444 (2019).
- Butman, B., Noble, M. & Folger, D. W. Long-term observations of bottom current and bottom sediment movement on the mid-Atlantic continental shelf. J. Geophys. Res. 84, 1187 (1979).
- 31. Johnson, H. P. et al. Anomalous concentration of methane emissions at the continental shelf edge of the northern Cascadia margin. *J. Geophys. Res. Solid Earth* **124**, 2829–2843 (2019).
- 32. Riedel, M. et al. Distributed natural gas venting offshore along the Cascadia margin. *Nat. Commun.* **9**, 3264 (2018).
- Merle, S. G. et al. Distribution of methane plumes on Cascadia margin and implications for the landward limit of methane hydrate stability. Front. Earth Sci. 9, 104 (2021).
- Phrampus, B. J., Harris, R. N. & Tréhu, A. M. Heat flow bounds over the Cascadia margin derived from bottom simulating reflectors and implications for thermal models of subduction. *Geochem. Geophys. Geosyst.* 18, 3309–3326 (2017).
- Feng, X. et al. ¹⁴C and ¹³C characteristics of higher plant biomarkers in Washington margin surface sediments. *Geochim. Cosmochim. Acta* 105, 14–30 (2013).
- Brothers, D. S. et al. Seabed fluid expulsion along the upper slope and outer shelf of the US Atlantic continental margin. Geophys. Res. Lett. https://doi.org/10.1002/2013gl058048 (2014).
- McGinnis, D. F., Greinert, J., Artemov, Y., Beaubien, S. E. & Wuest, A. Fate of rising methane bubbles in stratified waters: how much methane reaches the atmosphere? J. Geophys. Res. https://doi. org/10.1029/2005jc003183 (2006).
- 38. Yamamoto, A., Yamanaka, Y. & Tajika, E. Modeling of methane bubbles released from large sea-floor area: condition required for methane emission to the atmosphere. *Earth Planet. Sci. Lett.* https://doi.org/10.1016/j.epsl.2009.05.026 (2009).

- Kvenvolden, K. A., Lorenson, T. D. & Reeburgh, W. S. Attention turns to naturally occurring methane seepage. *Eos* 82, 457–457 (2001).
- 40. Saunois, M. et al. The global methane budget 2000-2012. *Earth Syst. Sci. Data* **8**, 697–751 (2016).
- 41. Etiope, G., Ciotoli, G., Schwietzke, S. & Schoell, M. Gridded maps of geological methane emissions and their isotopic signature. *Earth Syst. Sci. Data* https://doi.org/10.5194/essd-11-1-2019 (2019).
- 42. Archer, D., Buffett, B. & Brovkin, V. Ocean methane hydrates as a slow tipping point in the global carbon cycle. *Proc. Natl Acad. Sci. USA* **106**, 20596–20601 (2009).
- 43. Dyonisius, M. N. et al. Old carbon reservoirs were not important in the deglacial methane budget. *Science* **367**, 907–910 (2020).
- 44. Etiope, G. & Schwietzke, S. Global geological methane emissions: an update of top-down and bottom-up estimates. *Elementa* **7**, 47 (2019).
- 45. Kessler, J. D. et al. Basin-wide estimates of the input of methane from seeps and clathrates to the Black Sea. *Earth Planet. Sci. Lett.* **243.3–243.4**, 366–375 (2006).
- Pohlman, L. W., Ruppel, C., Boze, L. G. & Xu, X. Significant modern carbon present in microbial methane at gas seeps and gas charged sediments along the northern US Atlantic Margin. In *Proc. American Geophysical Union Fall Meeting*, OS23A-01 (AGU, 2021).
- Hornbach, M. J., Ruppel, C., Saffer, D. M., Van Dover, C. L. & Holbrook, W. S. Coupled geophysical constraints on heat flow and fluid flux at a salt diapir. Geophys. Res. Lett. https://doi. org/10.1029/2005gl024862 (2005).
- 48. Brothers, L. L. et al. Evidence for extensive methane venting on the southeastern US Atlantic margin. *Geology* **41**, 807–810 (2013).
- Joung, D., Ruppel, C., Southon, J. & Kessler, J. D. Elevated levels of radiocarbon in methane dissolved in seawater reveal likely local contamination from nuclear powered vessels. Sci. Total Environ. 806, 150456 (2021).

Publisher's note Springer Nature remains neutral with regard to jurisdictional claims in published maps and institutional affiliations.

Springer Nature or its licensor holds exclusive rights to this article under a publishing agreement with the author(s) or other rightsholder(s); author self-archiving of the accepted manuscript version of this article is solely governed by the terms of such publishing agreement and applicable law.

© The Author(s), under exclusive licence to Springer Nature Limited 2022

Methods

Samples were collected along the USAM and USPM from 25 August to 6 September 2017 and 27 May to 8 June 2019, respectively (Fig. 1). Sample collection sites on both ocean margins were chosen on the basis of previously determined seep locations and hydroacoustic imaging of water-column flares during the expeditions (Extended Data Figs. 1 and 3)^{15-19,31-33,36,47,48,50,51}. Many samples collected along the USAM were at sites with a total water-column depth greater than 300 m, including some greater than the nominal upper stability boundary for gas hydrates (550 m). By contrast, USPM samples were collected at sites shallower than 250 m, uniformly shallower than the upper stability boundary for gas hydrates⁶. Together, these sites represent seafloor seep CH₄ emissions that start near the shallow stability boundary for gas hydrates, enabling us to constrain the depth for which overlying surface waters are influenced by fossil CH₄.

The natural radiocarbon content of CH_4 dissolved in the waters of the USAM and USPM varied from ~0 to 750 pMC (Figs. 1 and 2 and Supplementary Tables 1 and 2), corresponding to CH_4 sourced from fossil carbon to contemporary carbon to anthropogenically influenced carbon with values above modern. Some of our $^{14}C-CH_4$ results were extremely high, displaying values up to four to five times those in the contemporary atmosphere (135 pMC) and more than two times previously reported values dissolved in ocean water (350 pMC in waters off Santa Monica²²). These values are probably affected by regional sources associated with nuclear power generation 49 .

Site description

Along both continental margins, numerous natural seafloor seeps are documented across a range of water depths (50 to >1,000 m) (refs. 15,16,18). Along the USAM, many CH4 seeps were found on the continental slope, some with depths greater than 1,000 m (refs. $^{47,48,50-52}$). The source of CH4 in these deeper depths is thought to be associated with geological features, such as gas pockets and diapirs 48 . Shallower seeps were also observed. Skarke et al. 18 found >500 seafloor seeps in depth ranges of 50–1,700 m between Cape Hatteras and Georges Bank, and these are are possibly sourced from gas pockets and hydrate dissociation (for water depths greater than 550 m). In addition, some seafloor bubble streams were very strong, with flares rising several hundred metres above the seafloor. The presence of authigenic carbonate rocks near the seep sites and analysis of their isotopic signatures suggest that these seeps have been active for thousands of years 18,52 .

Along the USPM, numerous CH₄ seeps have also been documented along the Washington and Oregon coasts, where they occur at a depth range from the deformation front at 3.000 m to the continental shelf <100 m^{16,17,19}. Johnson et al. ¹⁶ compiled previously published seep locations, as well as those discovered by commercial fishing boats, reporting the density of seafloor seeps as a function of site depth. The majority of the seeps (by numbers) reported by ref. 16 along the Oregon and Washington Cascade margin occurred at depths shallower than 250 m, too shallow to be associated with the dissociation of hydrates. However, when normalized with surface seafloor area, the highest density of seeps occurred between ~400 and 500 m depth, at or near the upper limit of gas hydrate stability, nominally 480 m in this region³⁴. We re-emphasize that our sample collections along the USPM were made at depths shallower than 250 m, and thus the CH₄ we collected in these waters was not likely associated with hydrate dissociation unless transport from deeper-water locations occurred during these collections.

Sample collection

We collected 39 samples during this study. Along the USAM, 17 samples were collected at different water depths from 4 sites mostly within or near the submarine canyon systems. Stations T6S1 and T7S1 were in and near Norfolk Canyon, T3S2 was in Keller Canyon offshore of Cape Hatteras and T1S2 was north of Washington Canyon. Three of these sites were chosen due to the known presence of gas seepage (T1S2,

T3S3 and T6S1); the other site (T7S1) was chosen due to the absence of acoustically detected gas seeps. The total water-column depth of three sites (T3S3, T6S1 and T7S1) ranged from 446 to 557 m, similar to the upper stability boundary for gas hydrates (~550 m); the deepest radiocarbon samples collected at these sites were 400 m below the sea surface. T1S2 was significantly shallower than the other USAM sites, with a total water-column depth of 288 m, but in an area of pervasive CH₄ seepage^{13,28}. All samples were collected on the RV Hugh R. Sharp from 25 August to 6 September 2017. Along the USPM, 22 samples were collected, 10 from 4 vertical water-column profile sites and 12 from surface-only sites located offshore of northern Oregon and Washington, USA. In addition, three samples were collected from the Salish Sea and the Strait of Juan De Fuca. The USPM samples were collected on board the RV Rachel Carlson during 27 May-8 June 2019. Because the RV Rachel Carlson is not equipped with a dynamic positioning system that could minimize vessel drift during our 3-4 h sampling periods, some bottom-water samples were collected at a depth tens of metres from the seafloor (for example, 26 m from the seafloor in Stn 4).

Radiocarbon isotope analysis for CH_4 is composed mainly of three steps: field sample collection at sea, purification and isolation in a land-based laboratory, and measurement via mass spectrometry. The procedures, materials and validation experiments for the field sample collection and laboratory purification procedures are fully described in refs. 24,29,53 .

In brief, gases dissolved in seawater are extracted on board the ship using suction hoses, a water pump, nylon and membrane filters, a vacuum pump, a gas-collection plastic bag, a compression pump and high-pressure gas cylinders (Extended Data Fig. 5). In this study, we used 7.62 cm (3 inches) diameter suction hose, which was sectioned into 10 m lengths and fitted with hose couplings so that sections could be combined relatively quickly. The combined hose was attached to the winch cable and slowly lowered to the targeted depth. On the ship, the end of the hose was connected to a high-performance water pump that can discharge up to 200-300 l min⁻¹. After the discharge pump, the water flows through three filters with different pore sizes (100, 50 and 10 µm, consecutively) to remove particles that can clog the gas-permeable membranes. The filtered waters are then flowed through high-performance gas-permeable membranes where a vacuum pump is simultaneously applied to the outside of the membranes to continuously extract the dissolved gases. The degassed waters were continuously discharged back to the ocean through a flow meter to monitor the volume of water processed. The extracted gases were then introduced to a gas-water separator, water condenser, and fresh silica gel trap to remove water droplets and vapour. The dry extracted gas was temporarily stored in a gas-collection plastic bag (~400 l) that was cleaned immediately before sample collection by flushing with both zero-air and sample gas. The extracted gases stored in the plastic bag were then compressed and finally stored in a small cylinder (~1.6 l), which housed roughly 220 l of extracted dissolved gases per sample. The small cylinders with extracted gases were transported to the land-based laboratory to further purify the gases, isolate the CH₄ and prepare it for isotopic analysis via accelerator and isotope ratio mass spectrometry. To minimize analytical error, sufficient CH₄ C (>200 µg C) was collected for a conventional-sized accelerator mass spectrometry analysis. Thus, at some surface-water sites with background CH₄ concentrations (~2 nM), we had to process over 35,000 l of seawater, taking over 3 h. Blank samples were collected at sea by filling the gas-collection plastic bag with ultra-high-purity zero-air and compressing that air into the small cylinder.

Because the extracted gases include other forms of carbon such as CO_2 , CO and non- CH_4 hydrocarbons, the extracted CH_4 must be purified in the land-based laboratory⁵³. All procedures are carried out under sub-ambient pressures, ensuring no ambient carbon is introduced into the system (Extended Data Fig. 5). The extracted gases in the cylinder are passed through a molecular sieve column to remove the majority of

CO $_2$. After the molecular sieve, the gases flow through liquid nitrogen (LN) traps, and the combination of both molecular sieve and the LN traps quantitatively removes CO $_2$ from the sample. After CO $_2$ removal, the gases are introduced to a combustion oven set at a temperature of 450 °C to convert CO and non-CH $_4$ hydrocarbons to CO $_2$, which can be removed by another LN trap located after the oven. At this point, all non-CH $_4$ carbon species are removed. The remaining CH $_4$ is then introduced to another oven set to 900 °C to covert CH $_4$ to CO $_2$ and H $_2$ O. The H $_2$ O produced from CH $_4$ combustion was isolated in a glass trap immersed in an ethanol and dry ice mixture, after which the CO $_2$ produced from CH $_4$ combustion was isolated in a glass trap immersed in LN. The CH $_4$ recovery was quantified by measuring the pressure and temperature of the combusted gas in a metal tube of known volume. The CO $_2$ collected from CH $_4$ combustion was transferred to a cleaned Pyrex tube and flame sealed for storage.

Two gas standards were used to monitor and assess the performance of vacuum line purification/combustion procedures. The concentrations of CO₂, CO and CH₄ in these gas standards were chosen to bound the typical concentrations observed in our samples (Extended Data Fig. 6). Standards were run after every 3-4 sample measurements. The processed standards were also collected and measured for radiocarbon. The total carbon background was also monitored daily by running zero-air for 1.5–2.0 h under the same procedures as samples. The total carbon background was always <0.004 μgC l⁻¹ during the entire sample purification periods (Extended Data Fig. 6). Finally, all the gas samples, including standards, were stored in flame-sealed Pyrex tubes and sent to the Keck Carbon Cycle AMS Laboratory at University of California, Irvine, where they were measured for radiocarbon and the stable carbon isotopes used for radiocarbon value corrections via accelerator mass spectrometry and isotope ratio mass spectrometry, respectively. All ¹⁴C values are reported in the pMC notation, which is corrected for isotopic fractionation using values of δ^{13} C as prescribed in ref. 54.

Discrete bottle samples for CH $_4$ concentrations were also collected at the same sites and depths as the 14 C-CH $_4$ samples and analysed following procedures presented in refs. 12,13,55 . Immediately after the sample collections, a 10 ml headspace of ultra-high-purity nitrogen was injected into each sample vial by displacing an equal volume of sample water. The water in each vial was sterilized by adding 100 μ l of saturated HgCl $_2$ solution. Samples were stored in an incubator set to a temperature of 4 °C for at least 12 h to allow dissolved gases to equilibrate with the headspace. The concentration of CH $_4$ in the headspace was determined using an Agilent 6850 gas chromatograph with a flame ionization detector (GC-FID).

Data availability

All data in this manuscript are available to the scientific community through the BCO-DMO database 56 and through other releases 15,57 . Source data are provided with this paper.

References

- Van Dover, C. L. et al. Blake Ridge methane seeps: characterization of a soft-sediment, chemosynthetically based ecosystem. *Deep Sea Res.* 1 50, 281–300 (2003).
- Ruppel, C. D. et al. in World Atlas of Submarine Gas Hydrates in Continental Margins (eds Mienert, J. et al.) 287–302 (Springer, 2022); https://doi.org/10.1007/978-3-030-81186-0_24
- 52. Prouty, N. G. et al. Insights into methane dynamics from analysis of authigenic carbonates and chemosynthetic mussels at newly-discovered Atlantic Margin seeps. *Earth Planet. Sci. Lett.* **449**, 332–344 (2016).

- Sparrow, K. J. & Kessler, J. D. Efficient collection and preparation of methane from low concentration waters for natural abundance radiocarbon analysis. *Limnol. Oceanogr. Methods* 15, 601–617 (2017).
- 54. Stuiver, M. & Polach, H. A. Discussion reporting of ¹⁴C data. *Radiocarbon* **19**, 355–363 (1977).
- 55. Weinstein, A. et al. Determining the flux of methane into Hudson Canyon at the edge of methane clathrate hydrate stability. *Geochem. Geophys. Geosyst.* 17, 3882–3892 (2016).
- Kessler, J. D. & Joung, D. Radiocarbon in Methane from Waters of the US Atlantic and Pacific Margins as Collected on R/V Hugh Sharp Cruise HRS1713 and R/V Rachel Carson Cruise RC0026 in 2017 and 2019 Version 1 (BCO-DMO, 2021); https://doi. org/10.26008/1912/bco-dmo.861576.1
- Baldwin, W. E. et al. Split-Beam Echo Sounder and Navigation Data Collected Using a Simrad EK80 Wide Band Tranceiver and ES38-10 Transducer During the Mid-Atlantic Resource Imaging Experiment (MATRIX), USGS Field Activity 2018-002-FA (USGS, 2021); https://doi.org/10.5066/P948VJ4X

Acknowledgements

D.J.J. thanks G. Kim and the Research Institute of Oceanography, Seoul National University, for the financial support. This work was possible due to the outstanding technical support from the officers and crew members of the RV *Hugh R. Sharp* and the RV *Rachel Carlson*. This research is funded to University of Rochester by the US National Science Foundation (OCE-1851402) and US Department of Energy (DOE) through DE-FE0028980. The USGS had funding from USGS-DOE interagency agreements DE-FE0026195 and 89243320SFE000013. Any use of trade, firm or product name is for descriptive purposes only and does not imply endorsement by the US government.

Author contributions

D.J.J., C.R., T.S.W. and J.D.K. designed the study, and J.S. measured $^{14}\text{C-CH}_4$ using the accelerator mass spectrometry (AMS). D.J.J. and J.D.K collected and prepared samples in the fields and laboratory. All authors equally contributed to the interpretation of the data and writing of this manuscript.

Competing interests

The authors declare no competing interests.

Additional information

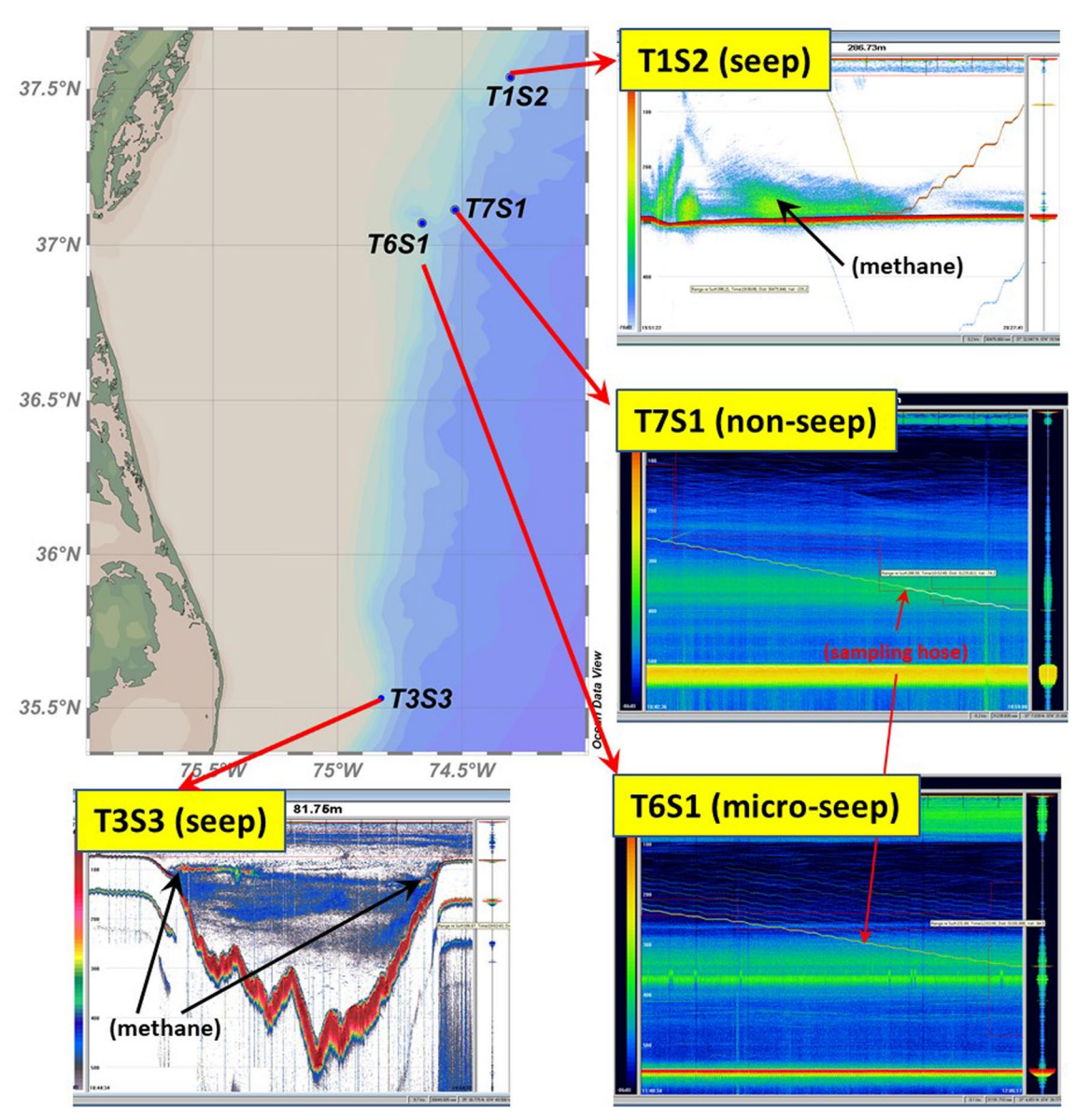
Extended data is available for this paper at https://doi.org/10.1038/s41561-022-01044-8.

Supplementary information The online version contains supplementary material available at https://doi.org/10.1038/s41561-022-01044-8.

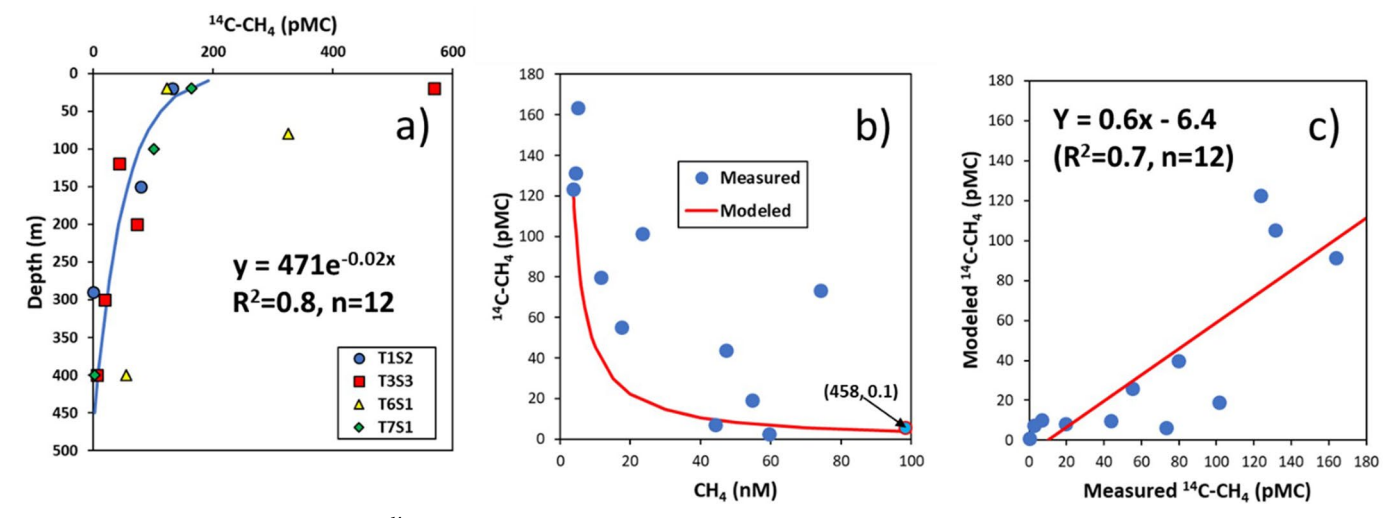
Correspondence and requests for materials should be addressed to DongJoo Joung.

Peer review information *Nature Geoscience* thanks Giuseppe Etiope, Jeanine Ash and the other, anonymous, reviewer(s) for their contribution to the peer review of this work. Primary Handling Editor: Xujia Jiang, in collaboration with the *Nature Geoscience* team.

Reprints and permissions information is available at www.nature.com/reprints.

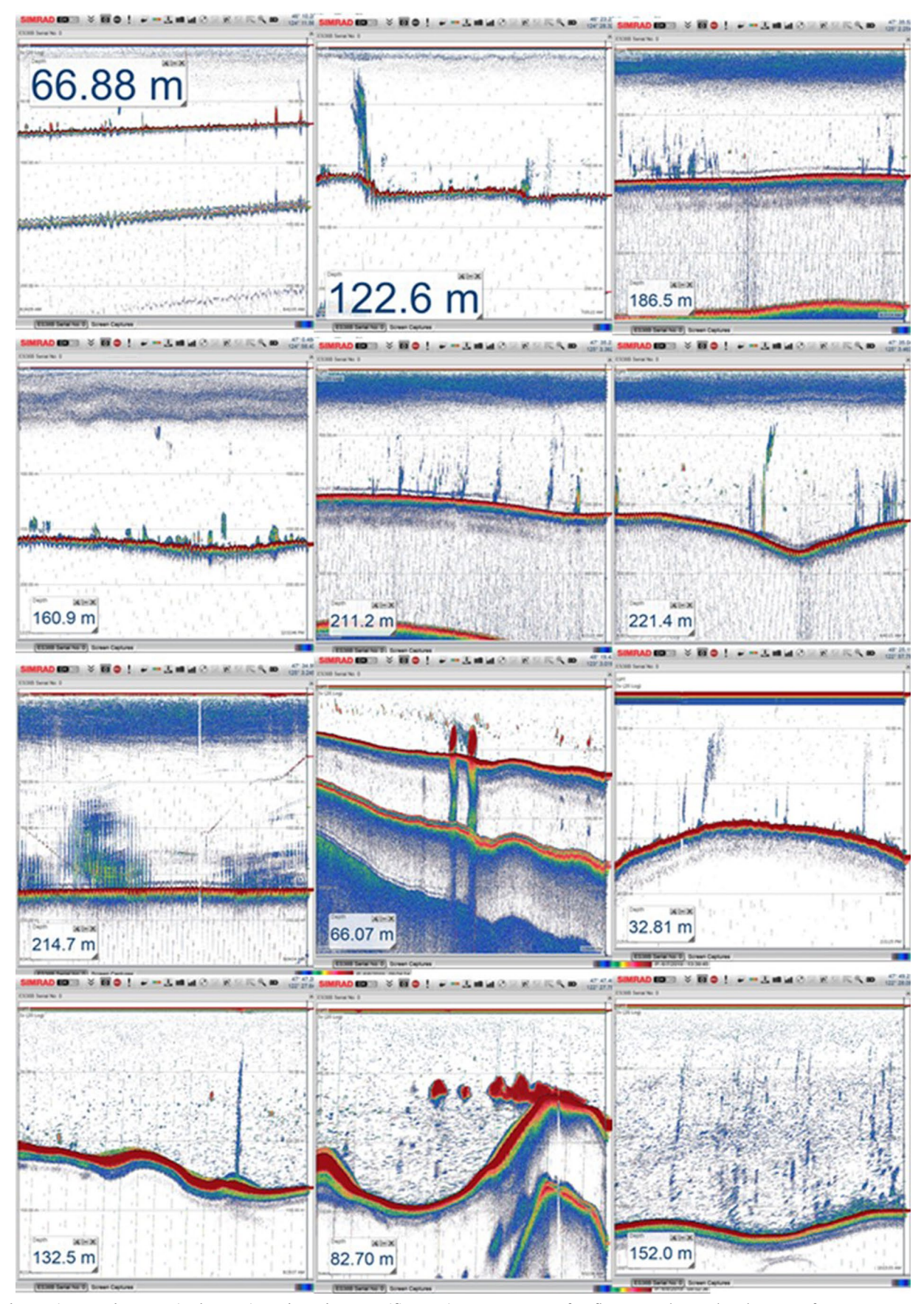


Extended Data Fig. 1 | US-Atlantic margin sampling stations with hydroacoustic data. Screen images of hydroacoustic data collected with a calibrated 38 kHz transducer on an EK60 split-beam sonar during the 2017 R/V Hugh Sharp cruise on the USAM. More information about data acquisition and the full dataset are available in refs. 15,57 .

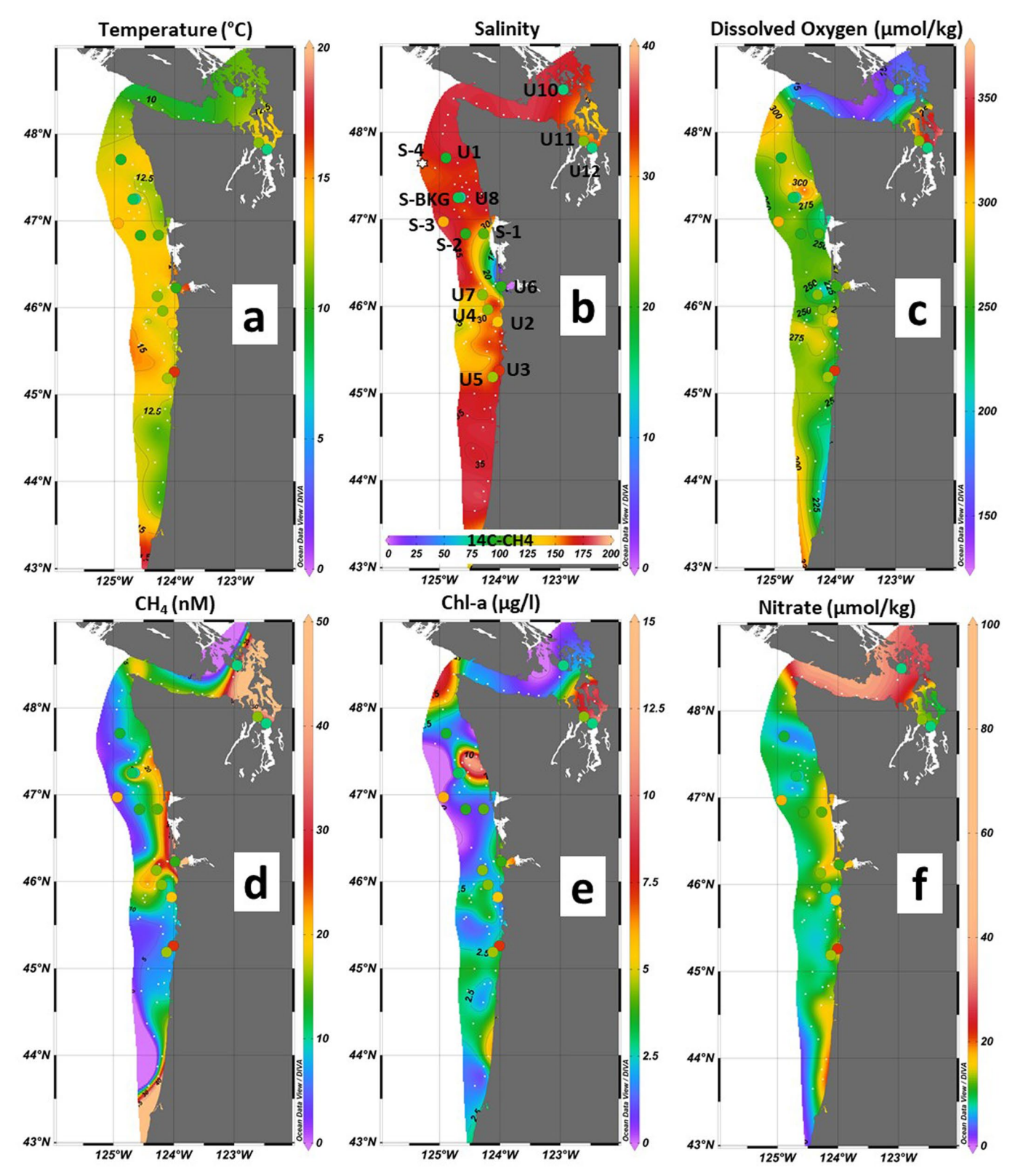


Extended Data Fig. 2 | Measurement data of 14 C-CH₄ for US-Atlantic margin along with mixing model results. Plots of (a) vertical profiles of 14 C-CH₄ and its relationship with depth from the US Atlantic margin, (b) the measured data (blue dots) and results from the two-endmember mixing model (red line) 14 , and (c) the comparison between the measured and mixing modeled 14 C-CH₄. For the

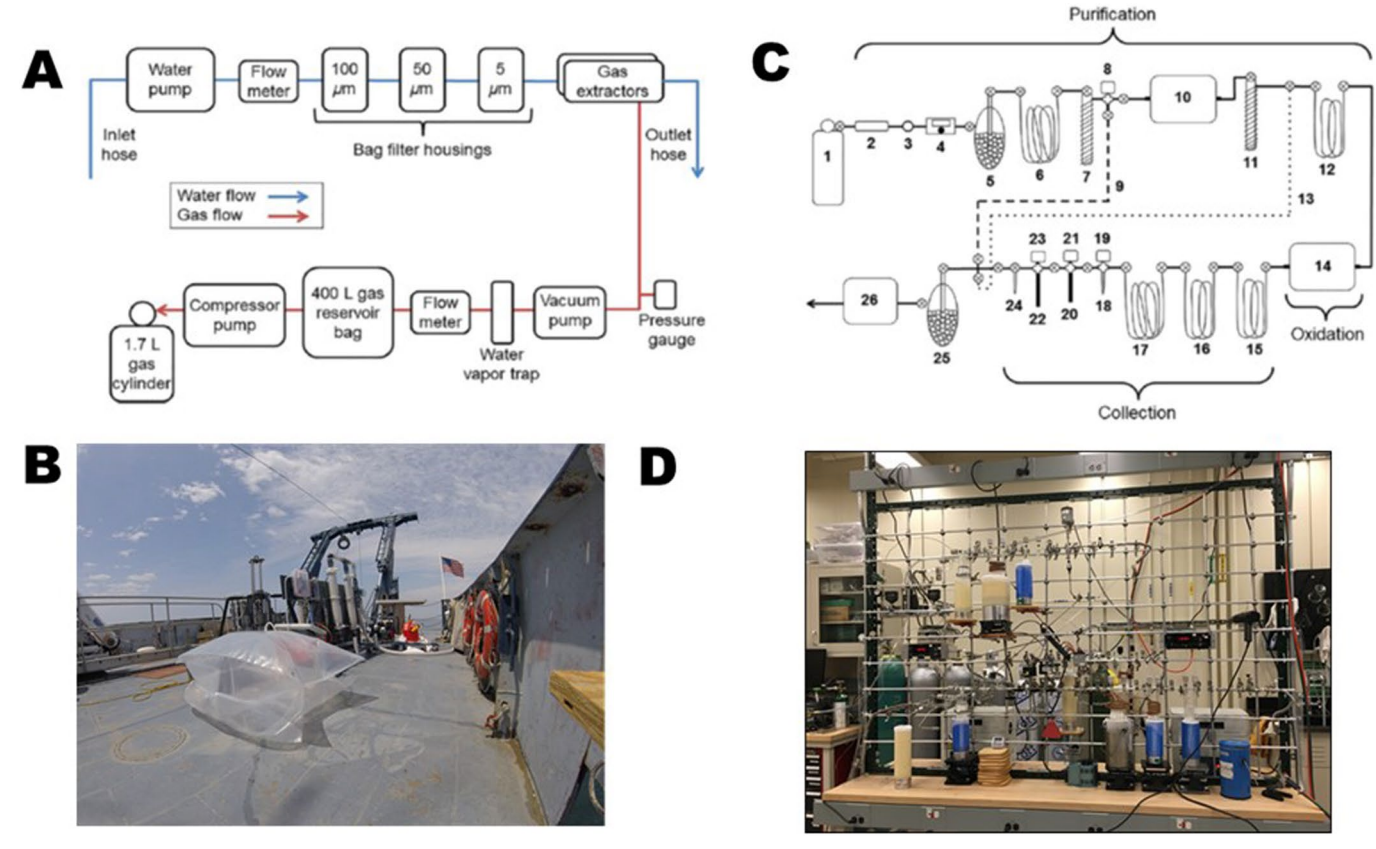
regression in (a), two data points, 570 pMC and 325 pMC from T3S3 surface and T6S150 m, respectively, were excluded due to the potential impact from local anthropogenic contamination from nuclear power generation. For figure (b), values in T1S2 (458 nM and 0.1 pMC) and T6S1 (3.7 nM, 123.4 pMC) were used for the bottom and surface endmembers, respectively.



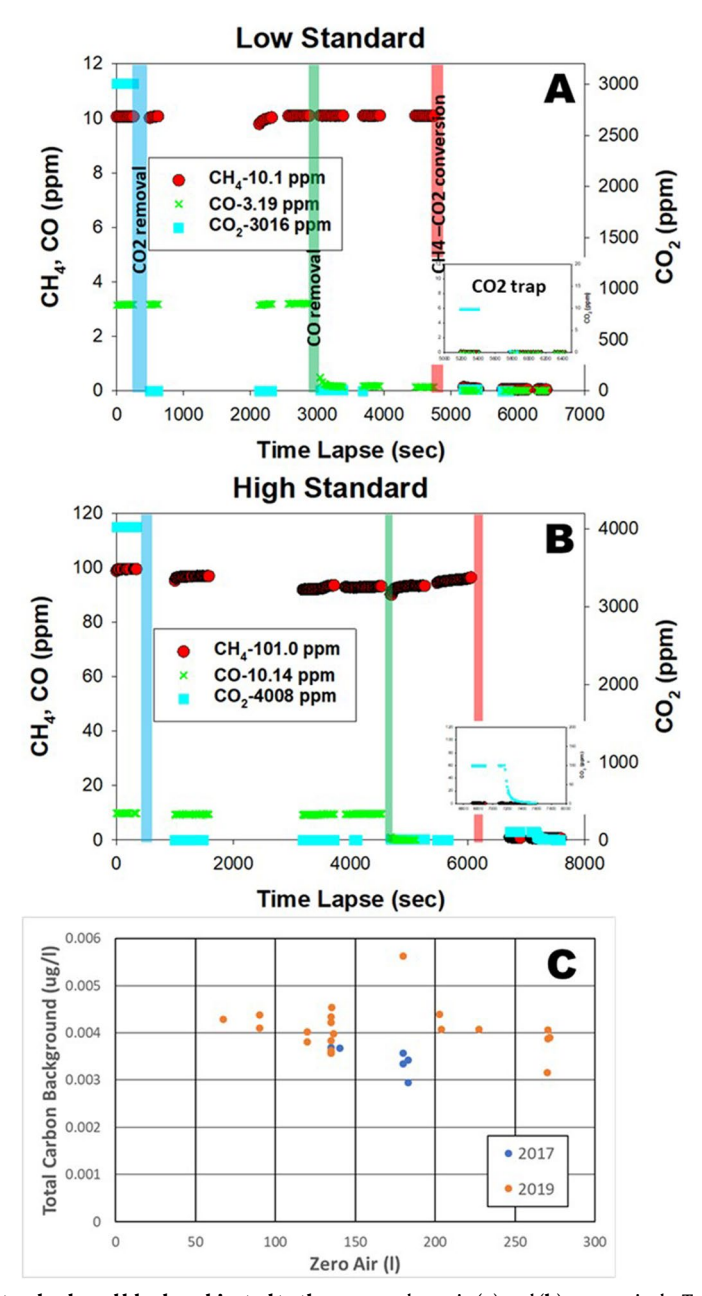
 $\textbf{Extended Data Fig. 3} | \textbf{Hydroacoustic observations along the US-Pacific margin.} \\ \textbf{Screen images of seafloor seeps detected on the US-Pacific margin using a hydroacoustic sensor (EK80) during the research cruise.} \\$



Extended Data Fig. 4 | **Surface distributions of water properties.** Surface contour plots of (a) temperature, (b) salinity, (c) dissolved oxygen, (d) CH_4 concentrations, (e) Chlorophyll a, and (f) nitrate concentrations (measured via Seabird Scientific, SUNA V2) in the Pacific margin. Colored dot represents $^{14}C-CH_4$, and the color scale and station ID are shown in (b).

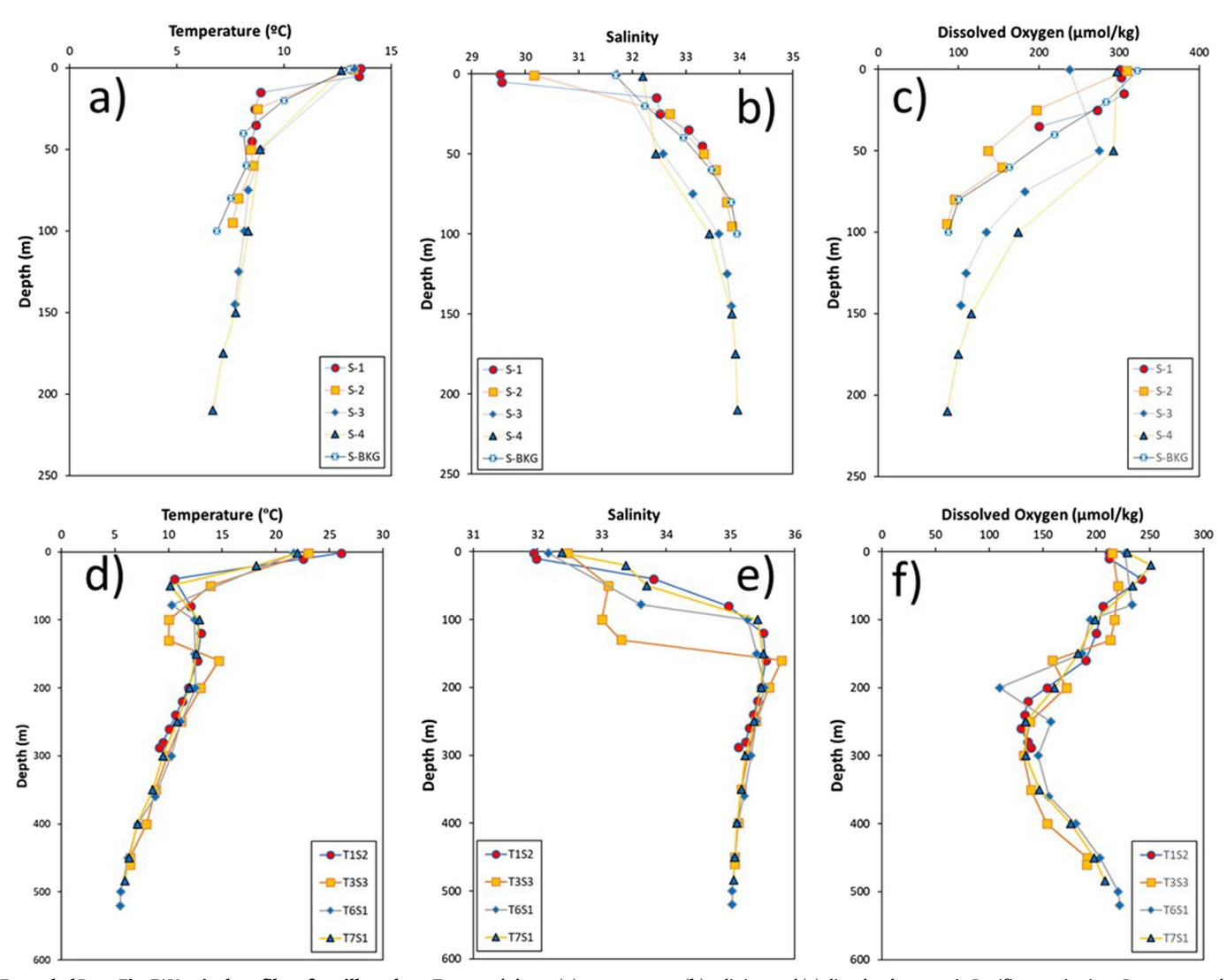


Extended Data Fig. 5 | Procedures for sample collection and preparation for measurement. Schematic diagrams of (a) gas extraction in the field and (c) gas purification in the laboratory. Pictures of equipment (b) in the field and (d) in the laboratory are also shown. Schematic diagrams (a and c) and photograph (d) were accessed from ref. ⁵³.



Extended Data Fig. 6 | Examples of gas standards and blanks subjected to the laboratory preparation procedures. Example diagrams for the gas standard tests monitoring the performance of the laboratory gas-purification system; High and low standards, which were customized based on the concentrations in the collected samples, were measured throughout this study, the results of which

are shown in (a) and (b), respectively. Total carbon blanks (c) for the purification system were also monitored daily when samples were run. Subplots in (a) and (b) show the trapping of CO_2 converted from CH_4 . Plots (a) and (b) were reproduced from ref. 29 .



Extended Data Fig. 7 | Vertical profiles of ancillary data. Top panel shows (a) temperature, (b) salinity, and (c) dissolved oxygen in Pacific margin sites. Bottom panel represents (d) temperature, (e) salinity and (f) dissolved oxygen in Atlantic margin sites.